



## Possible role of molecular clustering in single-file diffusion of mixed and pure gases in dipeptide nanochannels



Akshita R. Dutta<sup>a</sup>, Poorvajan Sekar<sup>a</sup>, Muslim Dvoyashkin<sup>a, b, c</sup>, Clifford Bowers<sup>b</sup>, Kirk J. Ziegler<sup>a</sup>, Sergey Vasenkov<sup>a, \*</sup>

<sup>a</sup> Department of Chemical Engineering, University of Florida, Gainesville, FL 32611, USA

<sup>b</sup> Department of Chemistry, University of Florida, Gainesville, FL 32611, USA

<sup>c</sup> Institute of Chemical Technology, Universität Leipzig, Leipzig, Germany

### ARTICLE INFO

#### Article history:

Received 6 December 2016

Received in revised form

5 April 2017

Accepted 11 May 2017

Available online 15 May 2017

#### Keywords:

Single file

Diffusion

PFG NMR

Clustering

### ABSTRACT

Single-file diffusion (SFD) of CO, CO<sub>2</sub>, and CH<sub>4</sub> gas molecules confined in L-Ala-L-Val nanochannels as both pure and binary mixtures is investigated using pulsed field gradient (PFG) NMR at the high field of 17.6 T. A unique SFD mobility is observed for each of the sorbates as pure gases. As binary mixtures, both sorbates exhibit identical SFD mobilities. The mixture mobilities were observed to be larger than those of the slowest-diffusing component in its pure form under the conditions when the total concentration of sorbate molecules in the channels was the same or comparable. It is proposed that molecular clustering in the studied channels is responsible for the relationship experimentally observed between the one-component and mixture mobilities. It is demonstrated that molecular clustering can also explain the lack of the experimental observation of a transition from the SFD mechanism to the center-of-mass diffusion mechanism, viz. diffusion mechanism characterized by correlated movements of all molecules in any particular channel.

© 2017 Elsevier Inc. All rights reserved.

## 1. Introduction

Single-file (SF) channels forbid molecules inside the channels from passing each other during a diffusion process by geometrically constraining them and, hence, conserving their relative order in the channels. A unique property of diffusion in sufficiently long SF channels is the growth of the mean square displacement (MSD) with the square root of time

$$\langle z^2(t) \rangle = 2Ft^{0.5}, \quad (1)$$

where  $F$  is the single-file mobility factor [1]. Diffusion in SF channels obeying Eq. (1) is known as single-file diffusion (SFD). In finite SF channels, however, the fastest and rate-determining diffusion mechanism in the limit of long observation times is related to correlated displacements of all molecules in each channel [1]. The direction of such correlated displacement at any particular time is expected to be independent of any previous displacement resulting

in the applicability of the Einstein relation, which requires a proportionality between the MSD and diffusion time. The diffusion associated with this type of displacements of chains of molecules is known as center-of-mass diffusion (COM). Theoretical and computational studies predict a transition from the SFD to COM diffusion regime, which is marked by a shift in the MSD dependence on diffusion time, at sufficiently large displacements [2–4]. However, until now, such a transition has not been observed experimentally.

We have recently reported the first experimental study of SFD of molecular mixtures [5,6]. The combination of high magnetic field (17.6 T) and large magnetic field gradients (up to 23 T/m) in this pulsed field gradient (PFG) NMR study allowed for measurement of MSDs of CO, CO<sub>2</sub>, and CH<sub>4</sub> molecules on a microscopic length scale as a function of diffusion time. Self-assembled L-alanyl-L-valine (AV) nanochannels were selected as model SF channels for the SFD observation of these gas molecules since the radius,  $r$ , of AV channels ( $r \sim 0.27$  nm) is smaller than the kinetic diameters,  $d$ , of these molecules ( $d_{\text{CO}} \sim 0.34$  nm,  $d_{\text{CO}_2} \sim 0.33$  nm,  $d_{\text{CH}_4} \sim 0.41$  nm) [7,8]. In the current paper, we provide a review of our SFD data for this sorbate/sorbent system together with the analysis of the relationship between the observed single-file mobilities of the pure gases and

\* Corresponding author.

E-mail address: [svasenkov@che.ufl.edu](mailto:svasenkov@che.ufl.edu) (S. Vasenkov).

their corresponding binary mixtures. We also discuss and explain the absence of a transition from the SFD to COM regime, which is predicted by the previously reported model [2,3] to occur under our experimental conditions.

## 2. Experimental

L-alanyl-L-valine crystallizes to form hydrophobic channels that have a helical structure. For this study, AV was purchased commercially from Bachem and used without further purification. The average length ( $l$ ) of the AV nanochannels was determined to be around 50  $\mu\text{m}$  from scanning electron microscopy images [9]. A fixed amount of AV crystals (~55 mg) was loaded into five-millimeter medium wall NMR tubes (Wilmad-LabGlass) that can sustain pressures up to 20 bar. The tubes were connected to a custom-made vacuum system and the samples were activated overnight at an elevated temperature of 373 K under high vacuum, i.e. at pressures below 0.001 mbar. Following activation, a measured mass of either pure gas or gas mixture was cryogenically condensed through the vacuum system and into the NMR tubes.

PFG NMR diffusion measurements were performed using a 17.6 T Bruker BioSpin NMR spectrometer operating at the  $^{13}\text{C}$  resonance frequency of 188.8 MHz. The diff60 diffusion probe was used to generate gradients in the range of 0.3–23 T/m. The 13-interval bipolar PFG NMR sequence with eddy current delays between 3.5 and 5 ms and sine-shaped gradients with the effective duration of 1.5–2.2 ms were used for all diffusion measurements [6,10,11]. This sequence was also used to estimate  $T_2$  and  $T_1$   $^{13}\text{C}$  NMR relaxation times for each sorbate by systematically changing the time interval between the first and second  $\pi/2$  rf pulse and the second and third  $\pi/2$  rf pulse, respectively, while keeping all other intervals constant. The  $^{13}\text{C}$   $T_2$  relaxation times of adsorbed CO, CO<sub>2</sub>, CH<sub>4</sub> molecules were estimated to be around 16, 18, and 22 ms, respectively. The corresponding  $T_1$  times were determined to be around 0.6, 2.7, and 1.5 s. All measurements were performed at 298 K.

The total pressure of the gas phase loaded into the five NMR tubes was around 10 bar at 298 K. In mixture samples, the partial pressure of each sorbate was 5 bar. Concentrations were obtained from the analysis of the recorded NMR spectra, as discussed in our previous work [5,6]. The measured concentration of each sorbate in each sample is presented in Table 1. This table shows that the total gas concentration in each of the samples is comparable, within the experimental uncertainty. This is significant as it allows us to directly compare the rates of diffusion of these molecules in single-sorbate and mixture samples.

Diffusion data is obtained from the change in PFG NMR signal intensity, which corresponds to the area under NMR lines, measured as a function of the applied magnetic field gradient while keeping all other parameters constant. The attenuation of the PFG NMR signal ( $\Psi \equiv \frac{S(g)}{S(g=0)}$ ) is plotted against  $q^2 t^{0.5}$ , where  $q$  is equal to  $2\gamma g \delta$ ,  $\gamma$  is the gyromagnetic ratio,  $g$  is the gradient strength,  $\delta$  is the effective gradient duration, and  $t$  is the diffusion time. Given the helical nature of the AV nanochannels and their random orientation

in the PFG NMR sample, the expectation of the signal attenuation for sorbates exhibiting SFD is given by:

$$\begin{aligned} \psi(q, t) &= \sqrt{\frac{p^2 \pi}{2q^2 \langle z^2(t) \rangle_{\text{helix}}}} \operatorname{erf} \left( \sqrt{\frac{q^2 \langle z^2(t) \rangle_{\text{helix}}}{2p^2}} \right) \\ &= \sqrt{\frac{p^2 \pi}{4q^2 F_{\text{helix}} t^{0.5}}} \operatorname{erf} \left( \sqrt{\frac{q^2 F_{\text{helix}} t^{0.5}}{p^2}} \right) \end{aligned} \quad (2)$$

where  $p$  is a geometrical factor that relates the actual MSD,  $\langle z^2(t) \rangle_{\text{helix}}$ , of molecules along the helical diffusion path with the observed MSD,  $\langle z^2(t) \rangle$ , and is equal to 1.3 [1,6,12].  $F_{\text{helix}}$  denotes the actual single-file mobility factor along the helical path of the AV channels. The dependence of the signal attenuation on  $q^2$  in Eq. (2) is different from the monoexponential dependence expected for normal diffusion without any diffusion anisotropy because this equation was developed for one-dimensional diffusion assuming a random distribution over the channel directions in a sample.

## 3. Results and discussion

The measured PFG NMR attenuation curves for diffusion of CO, CO<sub>2</sub>, and CH<sub>4</sub> in single-sorbate and mixture samples, as shown in Fig. 1, are scaled to test the agreement of the data measured at different diffusion times with Eq. (2) developed for SFD. The agreement with this equation, and thus the time scaling of MSD (Eq. (1)), is demonstrated by the observation that, for each sorbate and sample, the attenuation curves corresponding to different diffusion times coincide within the experimental uncertainty for a broad range of times used in the measurements.

For each gas in the single-component samples, a least-squares fit of Eq. (2) to all the attenuation curves in Fig. 1a measured for this gas at different diffusion times yielded a unique value of the single-file mobility,  $F_{\text{helix}}$ , which is presented in Table 2. Fig. 1b and c show coincidence of the attenuation curves of both sorbates in each of the two mixture samples, within the experimental uncertainty. Hence, a single least-squares fit by Eq. (2) is used to describe the attenuation curves for both molecules in each of the mixtures. The corresponding values of the single-file mobility of the mixture are shown in Table 2. The identical rates of transport observed for both sorbates in a mixture provides further confirmation for the SFD mechanism because this mechanism forbids the mutual passages of molecules in the channels. The small deviations observed between the experimental data and the least-squares fits (Fig. 1) can be assigned to differences between the actual channel orientation distribution and the completely random distribution assumption used to derive Eq. (2).

Fig. 2 a,b compares the time dependencies of MSDs obtained using Eq. (2) from the best-fits of the individual attenuation curves at every diffusion time for each sorbate in the single-sorbate and its corresponding mixture samples. The solid lines in the figure were obtained by fitting the time dependencies of MSD to Eq. (1), where  $\langle z^2(t) \rangle_{\text{helix}}$  and  $F_{\text{helix}}$  are substituted for  $\langle z^2(t) \rangle$  and  $F$ . The values of  $F_{\text{helix}}$  resulting from these MSD fits corroborate those reported in Table 2, within limits of the experimental error.

**Table 1**  
Gas concentration (mol/kg of AV) determined for each sample.

	CO	CO <sub>2</sub>	CH <sub>4</sub>	Total concentration in mixture samples
Single- Sorbate	0.56 ± 0.06	0.52 ± 0.05	0.48 ± 0.05	–
CO + CH <sub>4</sub>	0.34 ± 0.03	–	0.20 ± 0.02	0.54 ± 0.02
CO + CO <sub>2</sub>	0.24 ± 0.02	0.34 ± 0.03	–	0.58 ± 0.03

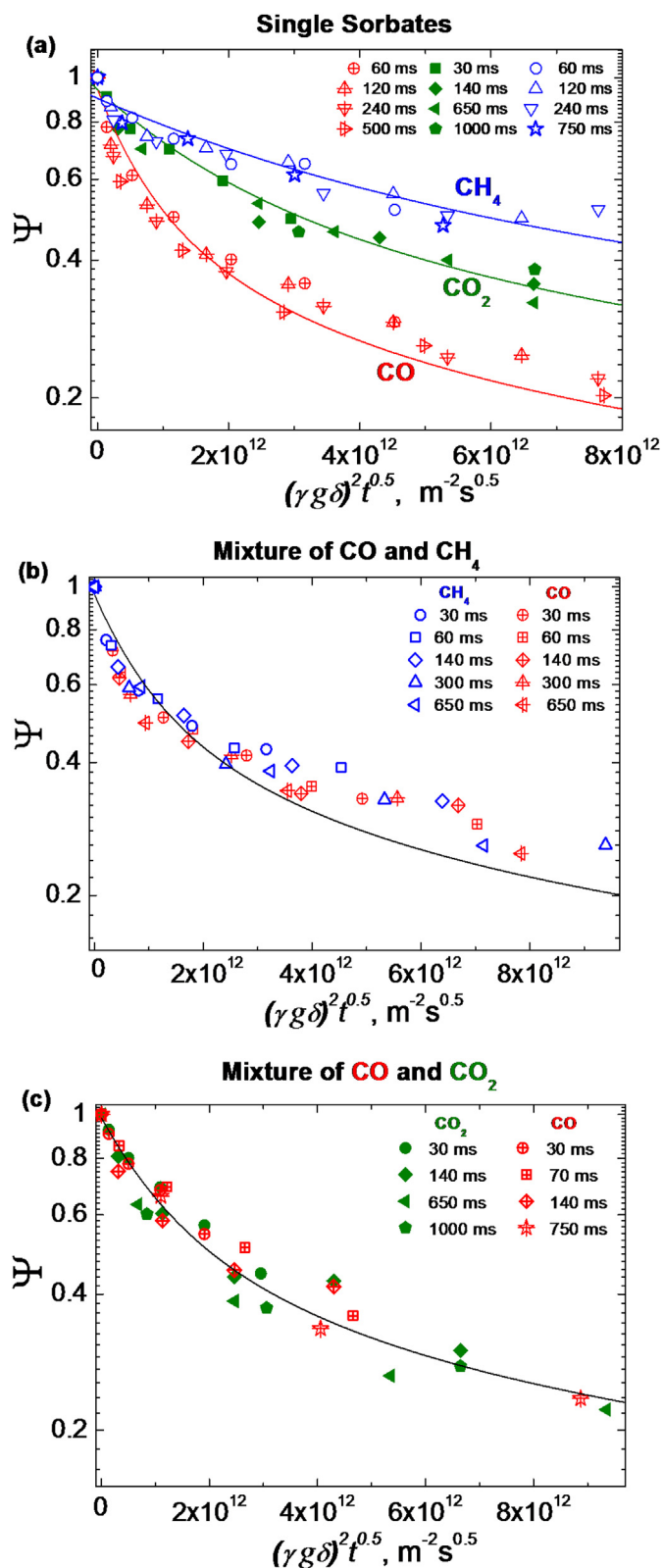


**Fig. 1.**  $^{13}\text{C}$  PFG NMR attenuation curves measured for gas diffusion in AV nanochannels at 298 K for samples loaded with (a) a single gas, (b) the CO/CH<sub>4</sub> mixture, and (c) the CO/CO<sub>2</sub> mixture. Solid lines are best-fit lines obtained using Eq. (2).

For each mixture the value of  $F_{\text{helix}}$  of two sorbates is found to be intermediate with respect to the single-file mobilities in the single-

**Table 2**

Single-file mobilities ( $F_{\text{helix}}$ ) obtained by least-square fitting of the attenuation curves in Fig. 1 using Eq. (2).

	CO <sub>2</sub>	CO <sub>2</sub> + CO	CO	CO + CH <sub>4</sub>	CH <sub>4</sub>
$F_{\text{helix}} \times 10^{13} \text{ (m}^2 \text{ s}^{-1/2}\text{)}$	$15.0 \pm 1$	$25 \pm 2$	$46 \pm 4$	$31 \pm 2$	$8.0 \pm 0.6$

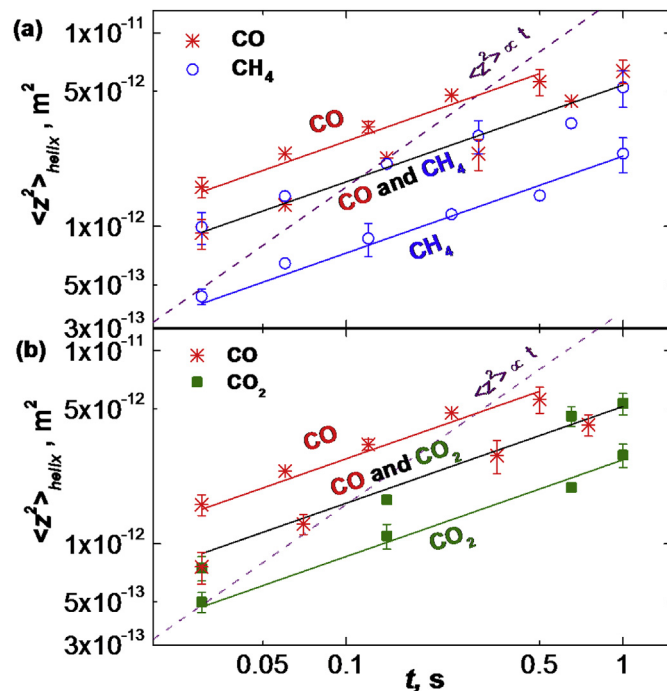


**Fig. 2.** The double-log plot of MSD dependence on diffusion time in AV nanochannels at 298 K for (a) CO, CH<sub>4</sub> and CO/CH<sub>4</sub> mixture, and (b) CO, CO<sub>2</sub> and CO/CO<sub>2</sub> mixture. The solid lines correspond to the time scaling of SFD (Eq. (1)). The dashed lines show the time scaling of normal diffusion.

component samples. This suggests that in a single-file system, the substitution of faster-diffusing molecules in place of slower-diffusing ones leads to a significant increase in the single-file mobility of the slower sorbate molecules, a trend which is in stark contrast with that typically observed for normal diffusion.

As briefly discussed in the introduction, computational and theoretical models of diffusion in SF channels of finite length predict a transition from the SFD to COM regime at sufficiently large displacements. The latter regime can be distinguished from the former one by the time scaling of the MSD, which in the COM regime is expected to be the same as for normal diffusion. A model of the single-file diffusion process that employs the random walk of particles with hard-core interactions predicts the transition to occur at the MSD given by Refs. [2,3].

$$\langle z^2(t) \rangle_{\text{COM}} = \left( \frac{1-\theta}{\theta} \right) \left( \frac{2l\lambda}{\pi} \right) \quad (3)$$

where  $\theta$  is the fractional loading of molecules in the channels,  $l$  is the channel length, and  $\lambda$  is the elementary displacement of diffusing species. Eq. (3) is used to estimate this crossover MSD for the systems studied here assuming that  $\lambda$  is determined by the collision diameter of diffusing molecules. Our previous publication provides a detailed description of how the parameters in Eq. (3) are estimated [5].

The values of crossover MSDs,  $\langle z^2(t) \rangle_{\text{COM}}$ , determined using Eq. (3) are given in Table 3. In all cases, this crossover value is less than

**Table 3**  
Estimates of fractional loadings ( $\theta$ ) used to predict the values of MSD ( $\langle z^2 \rangle_{\text{COM}}$ ) at which a transition from the SFD to COM diffusion regime should occur and the minimum cluster sizes estimated by Eq. (3).

	Single-Sorbate Samples			Mixtures	
	CO	CH <sub>4</sub>	CO <sub>2</sub>	CO + CH <sub>4</sub>	CO + CO <sub>2</sub>
$\theta$	0.20 ± 0.01	0.21 ± 0.01	0.18 ± 0.02	0.22 ± 0.02	0.16 ± 0.02
$\langle z^2 \rangle_{\text{COM}}$ (m <sup>2</sup> )	5.4 × 10 <sup>-14</sup>	6.2 × 10 <sup>-14</sup>	5.9 × 10 <sup>-14</sup>	5.6 × 10 <sup>-14</sup>	7.2 × 10 <sup>-14</sup>
Minimum cluster size (number of molecules)	110	30	50	140	70

the smallest MSD measured under our experimental conditions by PFG NMR. This implies that, for all samples reported here, a linear dependence of MSD on time should have been observed. The experimental data in Figs. 1 and 2, however, are not in agreement with this expectation. The incongruity between the experimental data and theoretical predictions can be resolved by considering the presence of long-range interactions between sorbate molecules. Such interactions could induce molecular clustering and this phenomenon has been demonstrated using molecular dynamics (MD) simulations of diffusion of similar gas molecules under single-file conditions [13–15].

In the scenario where individual molecules form large clusters that perform SFD, the actual elementary displacements,  $\lambda$ , in Eq. (3) is determined by the size of clusters, which is much larger than the collision diameter of the molecules used to estimate the crossover values shown in Table 3. This change in  $\lambda$  shifts the transition MSD to larger values for all samples studied. Hence, by assuming that the minimum crossover MSD is as large as the greatest experimentally measured MSD, Eq. (3) can be used to estimate the smallest cluster size for each system. The projected values of the minimum cluster sizes are reported in Table 3. They vary between 30 and 140 molecules, depending on the system.

The presence of molecular clustering in the context of single-file diffusion can also explain the relationship observed between the SFD mobilities of single-component sorbates and their mixtures. In accordance with the random walk model, the SFD mobility varies linearly with the product of  $\lambda$  and the square root of the diffusivity,  $D_0$ , of a single molecule/cluster in the infinite dilution limit [1].  $D_0$  is expected to be inversely proportional to  $\lambda$ , which is determined by the cluster size. Hence, the SFD mobility value should be proportional to the square root of  $\lambda$ . Therefore, it can be expected that the single-component sorbate that exhibits the largest SFD mobility (CO) forms larger clusters than its slower counterparts (CH<sub>4</sub> and CO<sub>2</sub>). One reason for CO molecules to form larger clusters than CH<sub>4</sub> and CO<sub>2</sub> can be related to dipole-dipole interactions between CO molecules. The average cluster in mixture samples would likely be intermediate in size with respect to their corresponding single-sorbate samples. This would translate into intermediate SFD mobilities of mixtures relative to their respective one-component sorbates, which is consistent with the experimental observations reported here. More studies are needed to investigate the molecular clustering in the studied systems. In particular, measurements of adsorption isotherms can be useful. It is discussed in ref. [16] that the shape of the adsorption isotherm can reveal the extent of interaction between molecules, especially if it exceeds their interaction with the host [16]. Such a strong interaction could result in clustering. While such an analysis can be insightful in general, the framework of AV nanochannels is flexible and can alter with loading resulting in adsorption isotherms that become difficult to interpret conclusively.

In addition to molecular clustering discussed above, the existence of strong transport barriers at the ends of AV channels [2,3] can be responsible for the absence of a transition to COM diffusion at the MSDs reported in Table 3. Such transport barriers,

however, are not expected to appreciably extend the length scale of the SFD regime. It is unlikely that the influence of transport barriers on the time scaling of MSD can exactly mimic that of SFD (Eq. (1)) for all pure and mixed sorbates studied in this work. However, additional theoretical studies are needed to clarify the contribution of transport barriers at channel boundaries to the transition from SFD to COM diffusion.

#### 4. Conclusions

Single-file diffusion of single-component gases and their binary mixtures in AV nanochannels was investigated by <sup>13</sup>C PFG NMR at a high magnetic field using large field gradients for a broad range of diffusion times. The SFD mechanism was confirmed by verifying the proportionality of the MSD with the square-root of time for each sorbate in both single-component and mixture samples. The SFD mobilities of both gases in the two-component mixture samples were found to be identical, which is consistent with the exclusion of mutual passages of molecules under the single-file conditions. At comparable total molecular concentrations in the channels, the mixture SFD mobilities were observed to be intermediate between their respective components' pure SFD mobilities. This relationship deviates from that observed for normal diffusion where the replacement of a fraction of a slower-diffusing component by a faster-diffusing one usually does not significantly influence the diffusivity of the former.

Simulation studies and theoretical considerations predict a transition from the SFD to COM regime at sufficiently large diffusion times. The crossover is characterized by a shift from the MSD dependence on the square root of time to a linear dependence on time. However, this transition to COM regime was not experimentally observed for any of the systems studied. Molecular clustering is proposed to explain the absence of this transition. Eq. (3) was used to estimate the minimum cluster size needed to sustain SFD under our experimental conditions. The clustering hypothesis was also used to qualitatively explain the unique relationship between the SFD mobilities of components in the single-sorbate and mixture samples. Our data suggest that molecular clustering in SF channels can be one of the main factors determining the rate of single-file diffusion of mixed and pure sorbates.

#### Acknowledgment

Acknowledgment is made to the Donors of the American Chemical Society Petroleum Research Fund for support of this research (PRF#53140-ND10). M.D. and A.D. acknowledge the financial support of this work by the NSF grant No. CHE-0957641 and the NSF CAREER award No. CBET-0957641, respectively. A portion of this work was performed in the McKnight Brain Institute at the National High Magnetic Field Laboratory's AMRIS Facility, which is supported by the National Science Foundation Cooperative Agreement No. DMR-1157490 and the State of Florida. The authors are grateful to Professor David S. Sholl, Georgia Institute of Technology, for his comments on this work.

**References**

- [1] J. Kärger, D.M. Ruthven, D.N. Theodorou, *Diffusion in Nanoporous Materials*, Wiley-VCH Verlag GmbH & Co. KGaA, Weinheim, Germany, 2012.
- [2] P.H. Nelson, S.M. Auerbach, *Chem. Eng. J.* 74 (1999) 43–56.
- [3] K. Hahn, J. Kärger, *J. Phys. Chem.* 102 (1998) 5766–5771.
- [4] J.-B. Delfau, C. Coste, M. Saint Jean, *Phys. Rev. E* 84 (2011) 011101.
- [5] A.R. Dutta, P. Sekar, M. Dvoyashkin, C.R. Bowers, K.J. Ziegler, S. Vasenkov, *J. Phys. Chem. C* 120 (2016) 9914–9919.
- [6] A.R. Dutta, P. Sekar, M. Dvoyashkin, C.R. Bowers, K.J. Ziegler, S. Vasenkov, *Chem. Commun.* 51 (2015) 13346–13349.
- [7] D.V. Soldatov, I.L. Moudrakovski, J.A. Ripmeester, *Angew. Chem. Int. Ed.* 43 (2004) 6308–6311.
- [8] N. Mehio, S. Dai, D.-E. Jiang, *J. Phys. Chem. A* 118 (2014) 1150–1154.
- [9] M. Dvoyashkin, A. Wang, A. Katihar, J. Zang, G.I. Yucelen, S. Nair, D.S. Sholl, C.R. Bowers, S. Vasenkov, *Microporous Mesoporous Mater.* 178 (2013) 119–122.
- [10] R. Mueller, S. Zhang, C. Zhang, R. Lively, S. Vasenkov, *J. Membr. Sci.* 477 (2015) 123–130.
- [11] R. Mueller, R. Kanungo, M. Kiyono-Shimobe, W.J. Koros, S. Vasenkov, *Langmuir* 28 (2012) 10296–10303.
- [12] M. Dvoyashkin, A. Wang, S. Vasenkov, C.R. Bowers, *J. Phys. Chem. Lett.* 4 (2013) 3263–3267.
- [13] D.S. Sholl, K.A. Fichthorn, *Phys. Rev. Lett.* 79 (1997) 3569–3572.
- [14] D.S. Sholl, *Chem. Phys. Lett.* 305 (1999) 269–275.
- [15] D.S. Sholl, C.K. Lee, *J. Chem. Phys.* 112 (2000) 817–824.
- [16] C. Chmelik, H. Bux, J. Caro, L. Heinke, F. Hibbe, T. Titze, J. Kärger, *Phys. Rev. Lett.* 104 (2010) 085902.